Supporting Information

S1 Python interface

The turbidostat software provides a simple python interface to allow the user to program control modules (modules that compute dilution rates).

Below is the stub code for the computeControl function. The computeControl function may make use of an optional state variable of user defined type State (or any builtin Python type). Each call to computeControl passes the exact State object that was returned by the last call thereby allowing a controller to keep state between function calls. Dilution rates computed by computeControl may also be functions of the OD, chamber, and current time.

```
class State:
  """ The state variable for the control function.

  This does not need to adhere to any proper interface although a
  readable __str__() method is highly recommended to allow for debugging.
  """

  def __init__(self):
    pass #any initialization code goes here

  def __str__(self):
    return " " #code for stringifying State goes here


def computeControl(self,od,z=None,chamber=0,time=0.0):
  """  Controller function

  self: self refers to the main controller object that contains
  all state such as the parameters file.  computeControl should never write
  to any members of self
  od: current od of the camber
  chamber: the chamber number indexed from zero
  time: the current time since start up.

  Returns: a tuple (list of dilution values for this chamber, state object)
  """

  #computation of dilution rate u, and state z goes here.
  return (u,z)
```

S2 Characterization Data

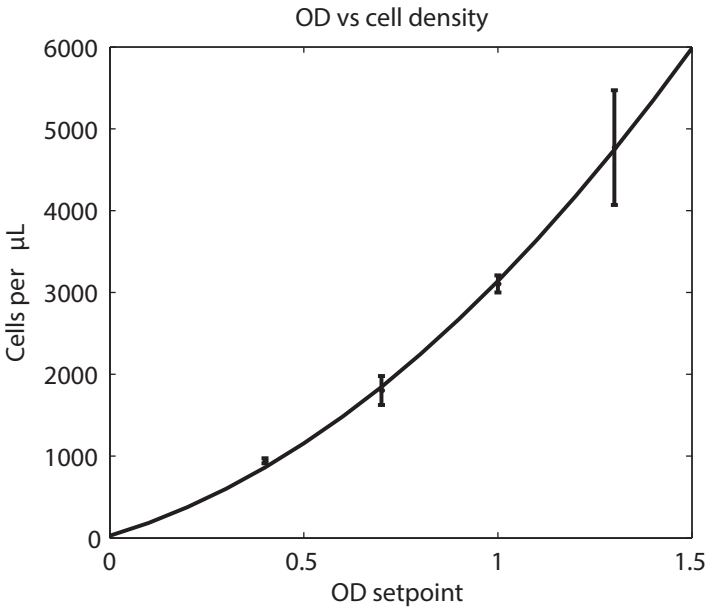

Figure S1: The relationship between measured OD and *S. cerevisiae* cell density with the second degree polynomial fit $f(x) = 1716x^2 + 1396x + 28$.

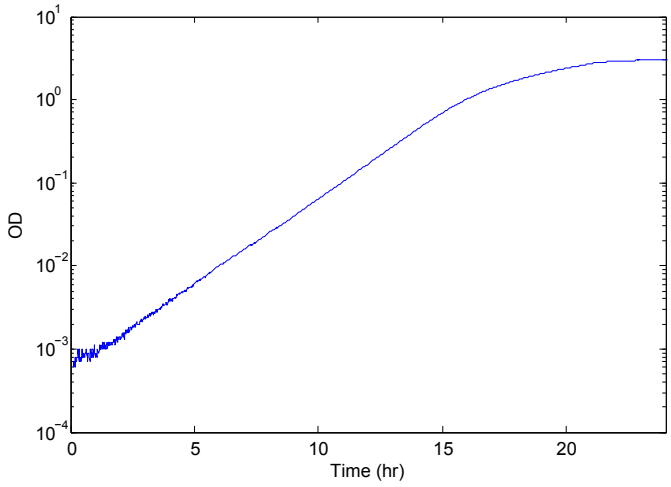

Figure S2: A typical growth curve as measured in our instrument. *S. cerevisiae* was grown in synthetic complete medium at 30 C and OD measurements were recorded once per minute. A growth rate of 0.485/hr (approx 86 minute doubling time) was fit to the exponential growth phase.

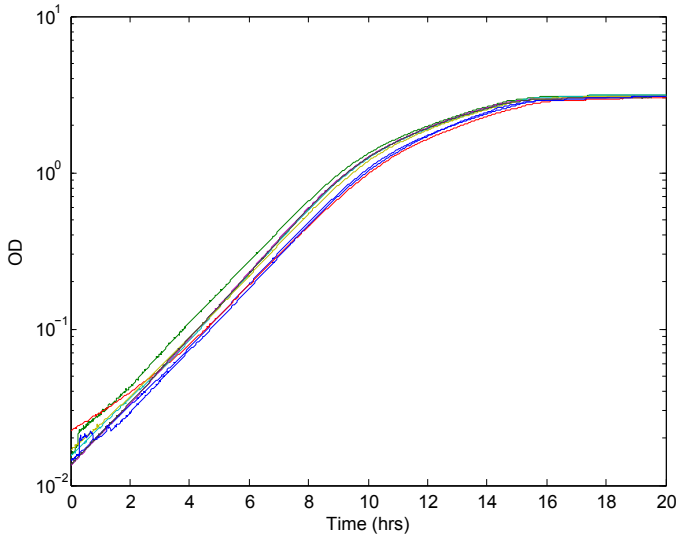

Figure S3: Eight simultaneous growth curves under the same conditions as in figure S2. Discrepancies between replicates can be explained by differences in inoculum volumes.

Table S1: Chamber by chamber for OD noise and pump rates. Open-loop STD measured in milli OD units represents the standard deviation of measurement noise in each chamber after the initial warm up period. The pump rate measurement is the average pump volume in micro liters per dispense unit using a NORM-JECT 3 ml syringe computed from the data in Figure S8. The pump rate STD is the standard deviation of the pump rates in figure S8 computed through bootstrapping.

	ch1	ch2	ch3	ch4	ch5	ch6	ch7	ch8
Openloop STD (OD$\times 10^{-3}$)	0.227	0.558	0.294	0.297	0.432	0.217	0.474	0.391
Pump rates (μL/unit)	0.49	1.47	1.37	1.51	1.6	1.58	1.58	1.53
Pump rate STD (nL/unit)	335.4	52	68.6	26.6	79.9	24.2	44.3	43.8

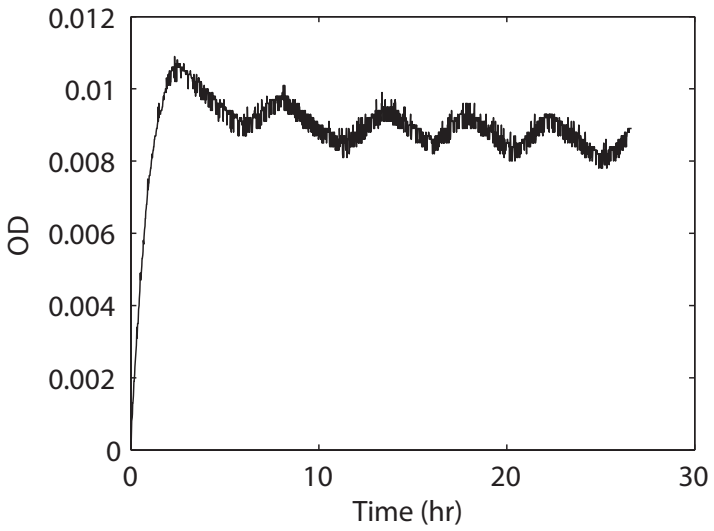

Figure S4: A typical measurement of OD noise for the first 24 hours of operation. The initial drift ($t = [0, 3]$) is caused by the device (primarily the laser diode) reaching thermal equilibrium and can be compensated for by a preheating period before blanking and inoculation. The remaining noise (t=[3,24]), consists of a slight decaying exponential, super imposed with high frequency noise and a slow ($T \approx 5$ hour) oscillation. The high frequency noise comes primarily form the light sensors, while the slight decay comes from the incubator recovering from light temperature overshoot (approx 0.2-0.3 C). The slow oscillations come from a slightly unstable incubator controller (± 0.1 C). The source of this instability likely comes from the heat propagation delay between the heating element through the water jacket to the temperature sensor. The primary source of temperature sensitivity comes from the laser diode. As with all diodes, the efficiency and therefor light output is negatively impacted by temperature. Previous design iterations that did not include a second photosensor for noise rejection where much more susceptible to temperature changes.

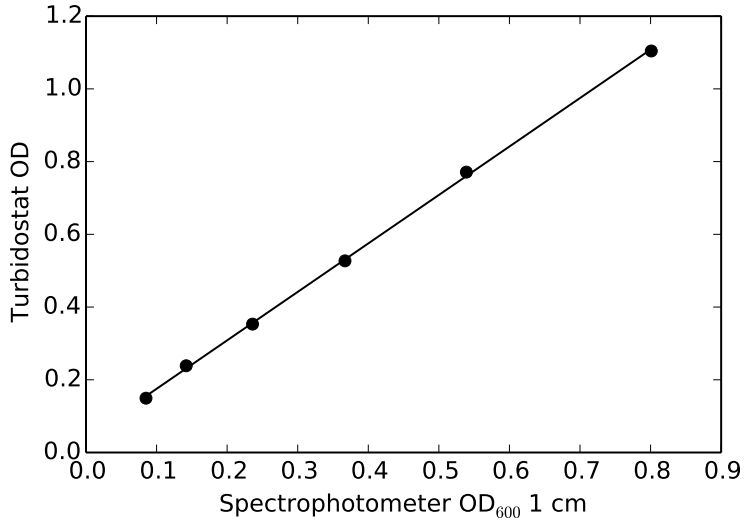

Figure S5: Spectrophotometer (Spec.) vs Turbidostat OD measurements. MG1655 derived *E. coli* strain BF003 was grown to stationary in M9 minimal medium and serially diluted in m9-salts. Each dilution was measured by both the turbidostat and the Edmunds Optics BRC111A-USB-UV/VIS spec. (dots). A constant conversion factor (Turbidostat/Spec) of 1.33 was then fit by linear regression (line).

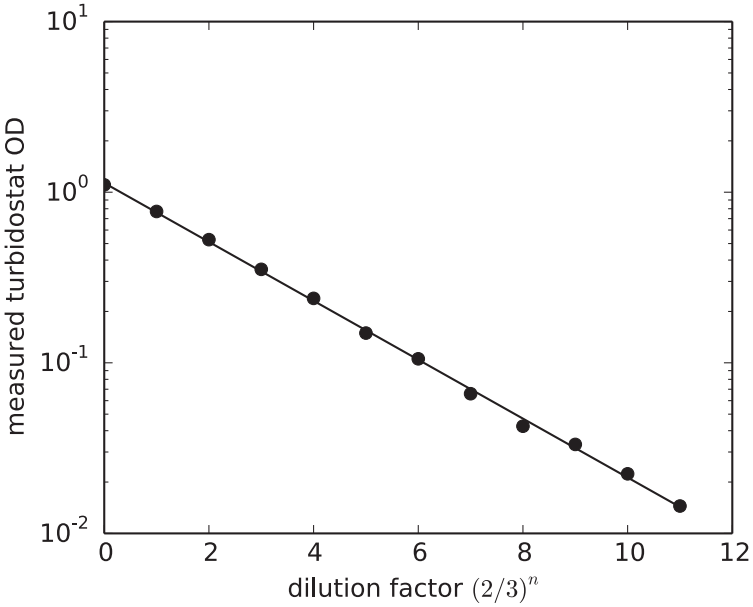

Figure S6: Twelve serial dilutions (1:2, M9-salts:culture) of the culture in figure S5 were measured in the turbidostat to demonstate linearity over two orders of magnitude.

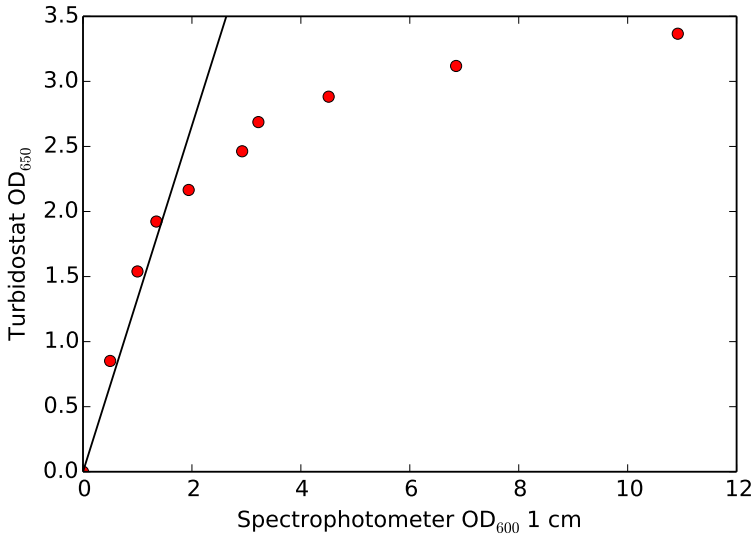

Figure S7: To determine the linear range of the device's absorbance measurement stationary phase *E. coli* was diluted from approximately OD_{600} 10 down to OD_{600} 0.5. These reference samples were measured both in our spectrometer (diluted into the linear range) and the turbidostat (undiluted) (red dots). Coplotting the points against the linear conversion factor computed in supplemental figure S5 we determined the linear range of our device to be between OD 0.0 and 2.0.

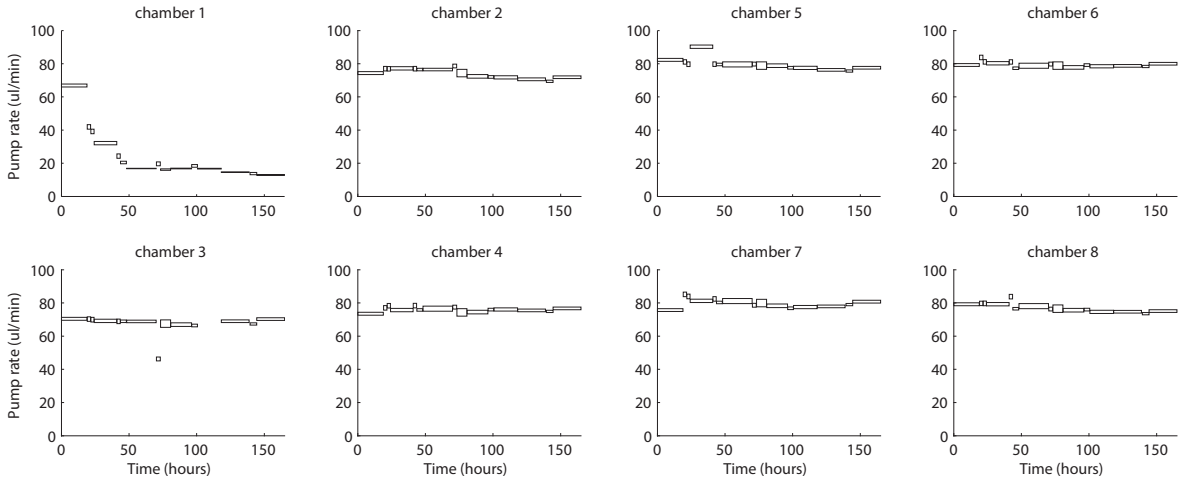

Figure S8: The chamber by chamber pump rates over a 160 hour period. The Turbidostat was set at a constant 50 unit dilution rate and effluent was periodically collected and measured in a graduated cylinder. The width of each box represents the collection time while the height represents the accuracy of the graduated cylinder used (i.e. one graduation). Chamber 1 is the first chamber to be dispensed into and is therefore the chamber that is subjected to hysteretic effects of the syringe plunger stretching. All experiments in this paper other than the one depicted here are preformed with an additional redispense step where 100units of media are pumped back into the media bottle. This redispense step fully compensates for all mechanical hysteresis.

S3 Parameter dependence on cell density

Table S2: Individual k_5 values for each experiment shown in figure 4c

k_5	Replicate 1	Replicate 2
Batch	0.0706	0.0608
OD 0.4	0.0407	0.0361
OD 0.7	0.0519	0.0537
OD 1.0	0.0795	0.0705
OD 1.3	0.1603	0.1711

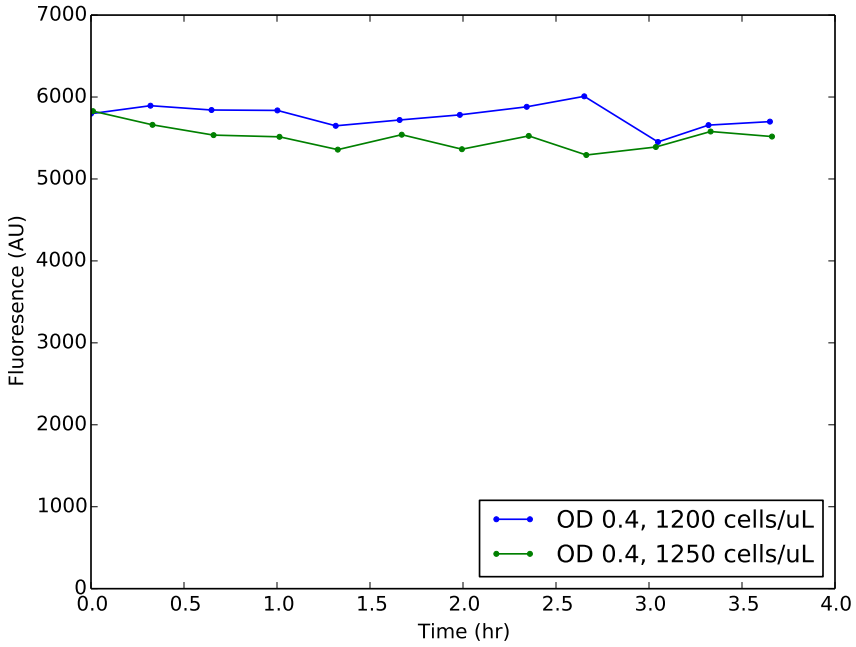

Figure S9: *S. cerevisiae* strain YKL73's steady state fluorescence (without auxin) showing no significant change in fluorescence without treatment over a multi hour timescale. YKL73 was grown in the turbidostat at OD 0.4 for 2 days prior to fluorescence measurement. An identical model but different cytometer was used to obtain this data making direct fluorescence comparison's impossible.

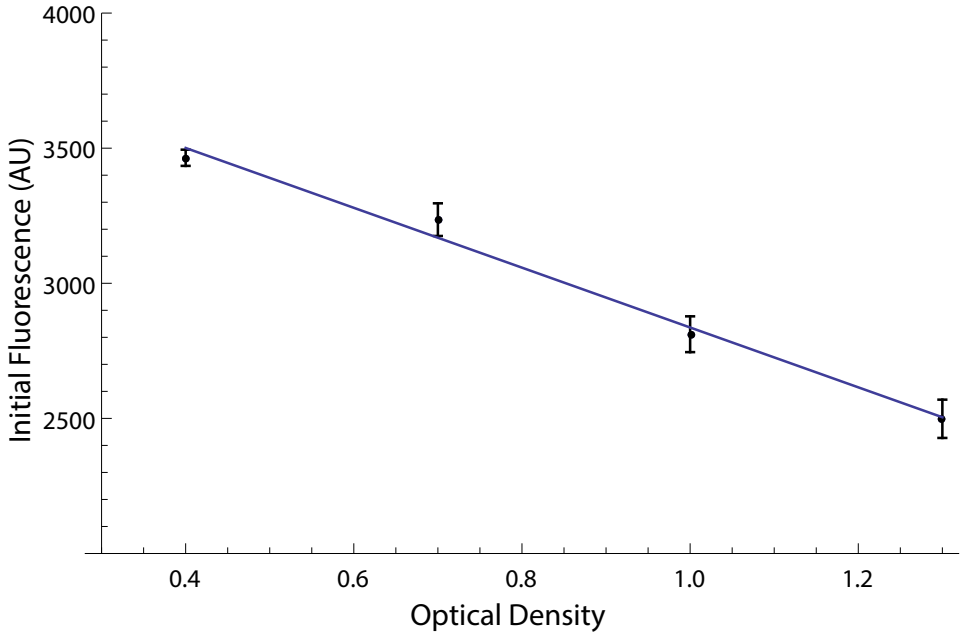

Figure S10: Initial fluorescence plotted as a function of OD for the data in figure 4b. The affine function $y = 3944 - 1107x$ was fit to the data.

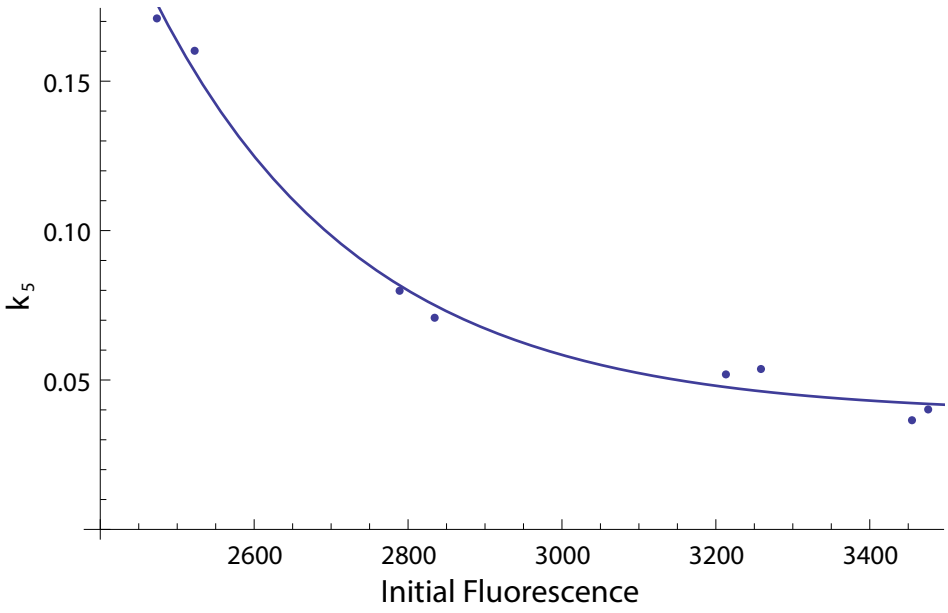

Figure S11: k_5 plotted as a function of initial fluorescence (dots). A fit was found to the exponential function $y = 0.03854 + 1210e^{-3.67\times10^{-3}x}$ (line).

S4 Fluorostat

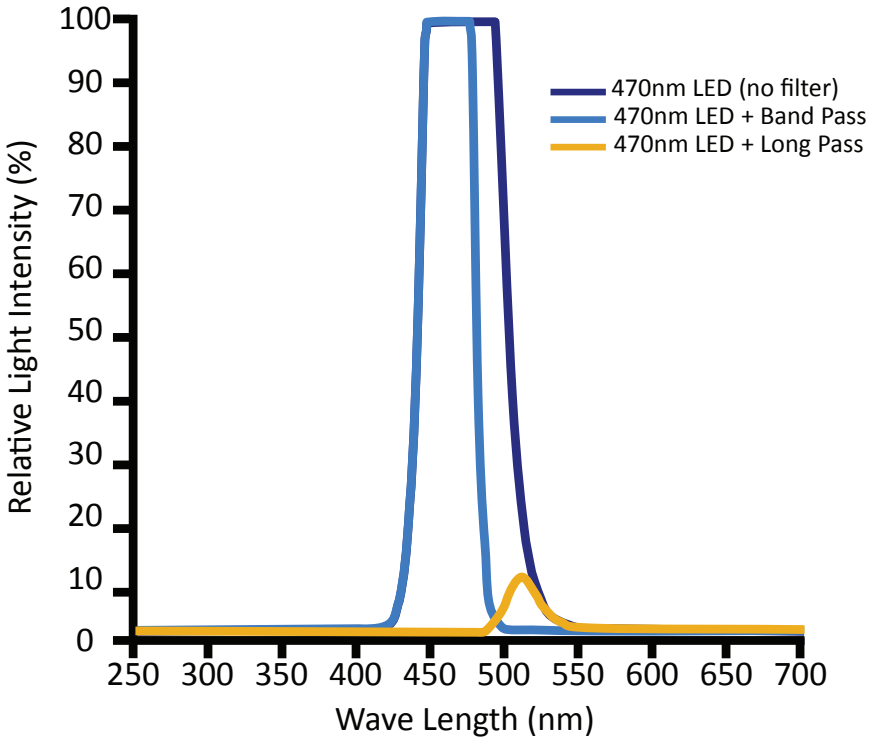

Figure S12: Measured spectrum of excitation LED (dark blue) through filters. The Bandpass filter removes longer wavelengths emitted by the LED (light blue) that have the potential to leak into the long pass filter's pass band (yellow). No significant light is transmitted though the combination of both filters allowing only light generated though florescence to be measured.

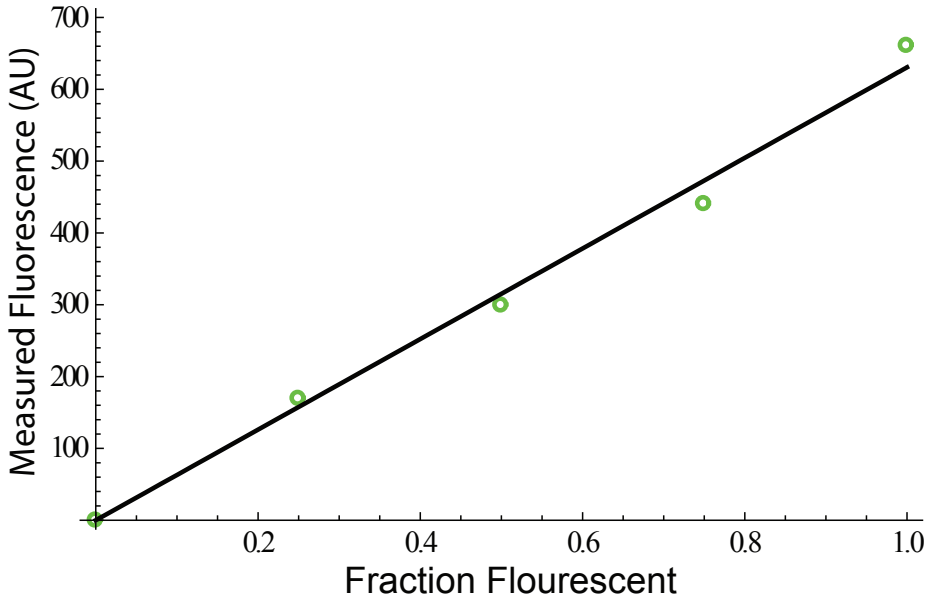

Figure S13: Stationary fluorescent *E. coli* were mixed with stationary wild type cells to create cultures of varying fluorescent intensity and measured in the fluorostat. Auto-fluorescence was determined by measuring the wild type cells and subtracted from each measurement (green circles). The points were then fit to a linear model (black line).

S5 3D models

All 3D models are available on the website.

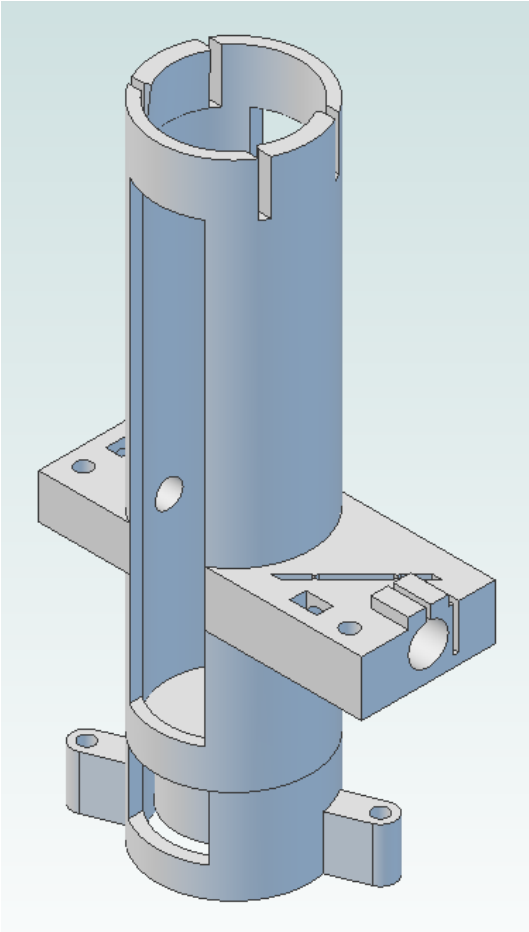

Figure S14: Drawing of all 3D printed parts in the main chamber assembly.

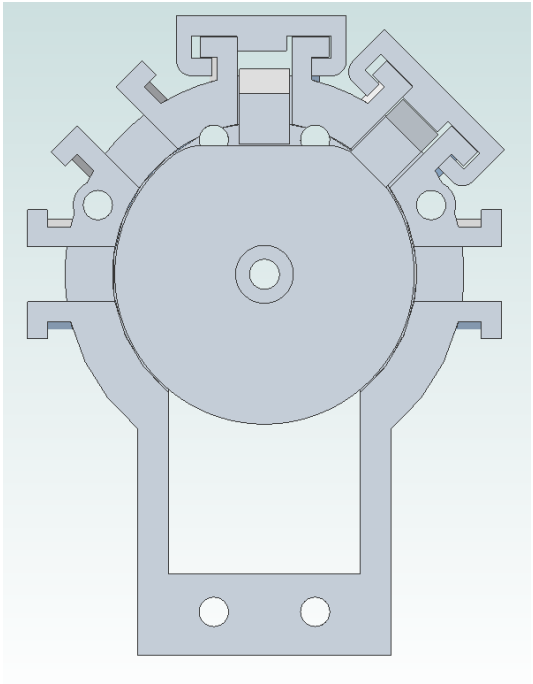

Figure S15: Drawing of 3D printed pinch valve assembly with face removed. The pinchers and center cam are laser cut from Delrin while all other parts are 3D printed. The left slot is normally left unused to provide a position where all valves are closed. Shown in the assembly are two assembled pinchers. The top pincher is in the open position while the upper right pincher is in the closed position. Tubes are fed through on the axis normal to the page.

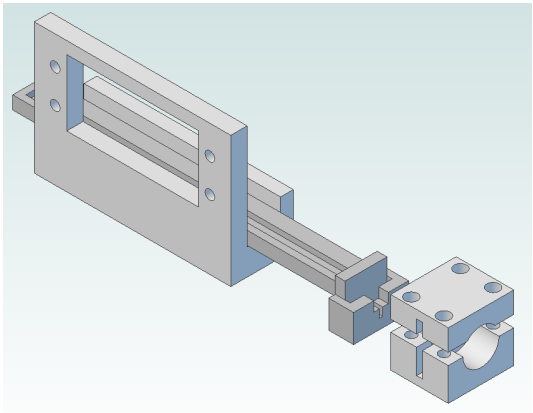

Figure S16: Drawing of the 3D printed syringe pump components. A servo motor actuates the slide attached to the syringe piston while the syringe body is clamped in place.

S6 Electrical Circuits

All circuits are available on the website and as supporting files.

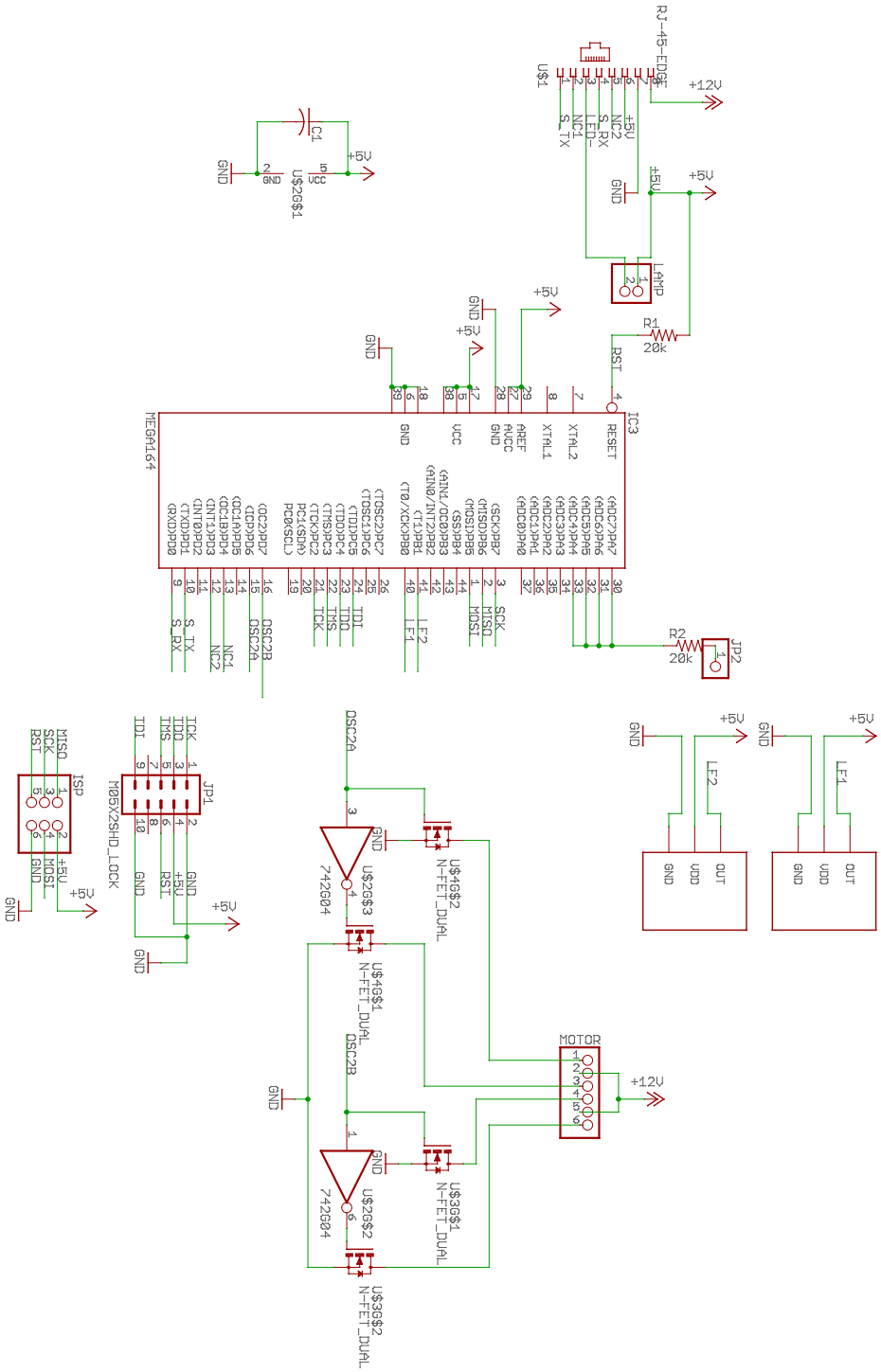

Figure S17: Schematic diagram for the chamber electronics. This circuit controls stirring speed and takes light measurements from each light sensor.

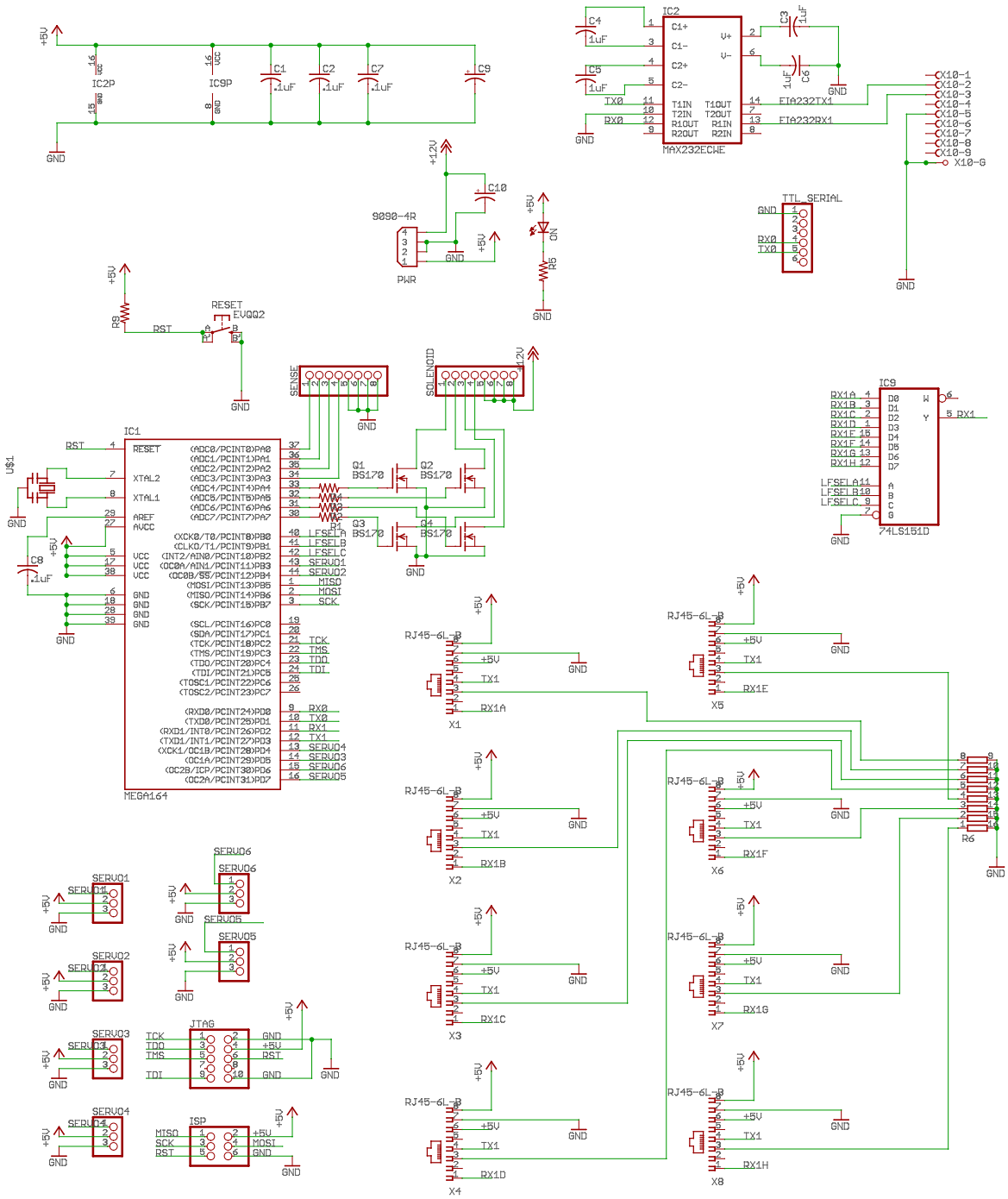

Figure S18: Schematic diagram for the main board electronics. The main board routes all communications between the chambers and controls all valves and pumps.